5-15-1993

Magnetization reversal in Co/Cr multilayer films

D. Wang
University of Nebraska - Lincoln

Roger D. Kirby
University of Nebraska-Lincoln, rkirby1@unl.edu

B. W. Robertson
University of Nebraska-Lincoln, brobertson1@unl.edu

David J. Sellmyer
University of Nebraska-Lincoln, dsellmyer@unl.edu

Magnetization reversal in Co/Cr multilayer films

D. Wang, R. D. Kirby, B. W. Robertson, and D. J. Sellmyer
Center for Materials Research and Analysis, and Departments of Physics and Mechanical Engineering, University of Nebraska, Lincoln, Nebraska 68588

Magnetization reversal of Co/Cr multilayer films is studied by utilizing initial magnetization curves, minor loops, isothermal and dc demagnetization remanence curves, and temperature dependence of the loops. Electron microscope observations reveal that the films consist of columnar grains of size from 400 to 800 Å. It is suggested that the magnetization reversal is dominated by rotation of single-domain grains. Numerical calculations are performed based on the Stoner–Wohlfarth coherent rotation model for noninteracting, single-domain particles of uniaxial anisotropy. The calculated results agree qualitatively with the experimental results. To investigate the quantitative differences, magnetic interactions among the grains are measured in terms of deviations from the linear Hankel plot predicted by Wohlfarth.

INTRODUCTION

It is well known that Co-based alloy films with Cr underlayers consist of columnar grains.[1] By changing the deposition conditions for the film and the Cr underlayer, the grain size in the lateral direction as well as the crystal texture can be well controlled. By multilayering films with nonmagnetic materials, an additional handle on the grain size in the film normal direction is obtained. This full control of the magnetic grain size makes it possible to tailor the magnetization behavior of the films. There has been much work on single-layer and some on multilayer films of Co-based systems[1,2] but there has been little discussion of the magnetization processes. It was shown that coercivities (H_c) as high as 1800 Oe can be obtained for Co/Cr multilayer films on a Cr underlayer.[3] In this work the magnetization behavior is studied by utilizing initial magnetization curves, minor loops, isothermal and dc demagnetization remanence curves from both thermally and field-demagnetized films, and the temperature dependence of the loops. The structural and microstructural properties obtained by SEM, TEM, and XRD are correlated to the magnetic properties by using the Stoner–Wohlfarth coherent rotation model for noninteracting single-domain particles of uniaxial anisotropy.[4]

FILM PREPARATION AND MEASUREMENTS

Co/Cr multilayer films were prepared in a multigun dc magnetron sputtering system. Films were deposited on copper and glass substrates which were mounted on a temperature-controlled electric heater. The base pressure was below 5×10^{-7} Torr and the argon pressure during sputtering was 10 mTorr. The thickness of the Cr underlayer was held at 4000 Å while the total Co thickness was kept at 600 Å. Individual layer thicknesses of the Co/Cr multilayers were controlled by programming the time that the substrate was stationary above the corresponding target. The crystal structure and texture were studied by x-ray diffractometry on a Rigaku DMAXB system and the layer structure was checked by small-angle diffractometry on the same system. Microstructure was studied by using a Jeol-840A SEM and a Jeol-2010 TEM. Magnetic properties were studied by using a MicroMag Alternating Gradient Force Magnetometer (AGFM) with a maximum field of 14 kOe, a VSM with maximum field of 17 kOe at room temperature, and a SQUID with a maximum field of 55 kOe at various temperatures. The fully automated AGFM with its high sensitivity (10^{-8} emu) allowed us to measure remanence curves accurately.

EXPERIMENTAL RESULTS

As we reported earlier[3] the Cr underlayer has bcc crystal structure and the Co layers have hcp structure for Co/Cr multilayer films on Cr underlayers. The bcc Cr underlayer is aligned with (100) crystal planes in the film plane. The hcp Co layers are preferentially aligned with (110) in the film plane. So the c axis, which is the easy magnetic axis, is in the film plane and presumably random-oriented in the film plane. Small-angle XRD shows only the first-order peak for typical films, indicating a measurable composition modulation but not sharp interfaces.

Of those samples mentioned in Ref. 3 particular films of (Co200 Å/Cr50 Å)*3 with a 4000 Å Cr underlayer are investigated further here. The microstructure was studied by both SEM and TEM. A SEM image on a fracture perpendicular to the surface of the film is shown in Fig. 1(a). The columnar structure is clearly seen to extend throughout the Cr underlayer and the multilayer region. Bright field TEM images such as Fig. 1(b) indicate that the grain size ranges from 400 to 800 Å. Similar results are obtained for a film deposited on glass substrate.

Figure 2 gives a room temperature loop and initial magnetization curves with field applied in the film plane. The two initial curves for the thermally demagnetized and field-demagnetized states are almost identical. The temperature dependence of M_s, H_c, anisotropy field H_k, and squareness S are shown in Fig. 3. The minor loops measured at room temperature are shown in Fig. 4.

DISCUSSION

For a nucleation type of magnetization reversal mechanism the two initial curves from thermally demagnetized and field-demagnetized should be very different. This is not the case as shown in Fig. 2. And the shape of our measured initial curves is different from that of typical nucleation

 0021-8979/93/106353-03$06.00

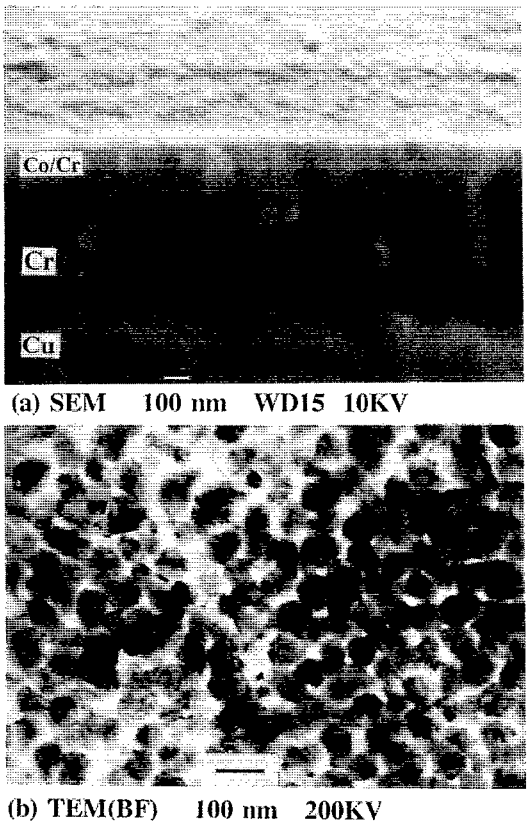

FIG. 1. (a) Secondary electron SEM micrograph with 65 deg tilt from the film normal; (b) bright field TEM micrograph using 200 keV for a film of (Co200 Å/Cr50 Å)**3 with a 4000 Å Cr underlayer on Cu substrate.

type of sintered $Nd_2Fe_{14}B$ magnet for which the magnetization rises much faster up to saturation at a field well below H_c.[5] The shape of the initial curve is also different from the case of typical pinning behavior[6] where the magnetization is close to zero until the field almost reaches H_c.

Kronmüller *et al.*[7] have studied magnetization reversal and found a similar formula for both pinning and nucleation mechanisms:

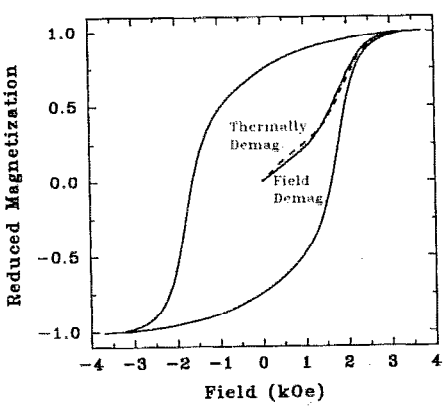

FIG. 2. Hysteresis loop and initial curves for the film in thermally demagnetized and field-demagnetized states.

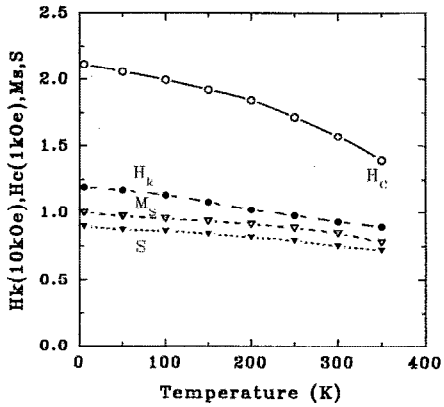

FIG. 3. Temperature dependence of H_c, H_k, M_s, S.

$$H_c = \alpha 2K/M_s - N_{\text{eff}} M_s , \tag{1}$$

here K is the anisotropy constant and N_{eff} the effective demagnetization factor. α is mechanism dependent and a function of misalignment, fluctuations of anisotropy, and exchange coupling. We tried to fit the experimental data shown in Fig. 3 to these models assuming a pinning mechanism for small or large pinning centers as well as a nucleation mechanism. The fits in each case were poor, indicating these models are inadequate here. Furthermore Cook and Rossiter[5] discussed the minor loops for pinning and nucleation mechanisms but the data shown in Fig. 4 are not similar to either.

Sagawa and co-workers[8] have reported that the critical sizes of single-domain particles for typical uniaxial permanent magnets range from about 0.3 to 1.6 μm. For a rough estimate we assume the proportional relationship[4]: $D_c \propto \gamma / M_s^2$, where D_c is the critical size for single-domain particle, γ is domain wall energy density, and M_s is the saturation magnetization; this results in a D_c of about 1000 Å for our films. Comparing with the measured grain size of about 600 Å it is likely that our films consist of single-domain grains thus the rotation of single-domain grains with uniaxial anisotropy is likely the dominant mechanism here.

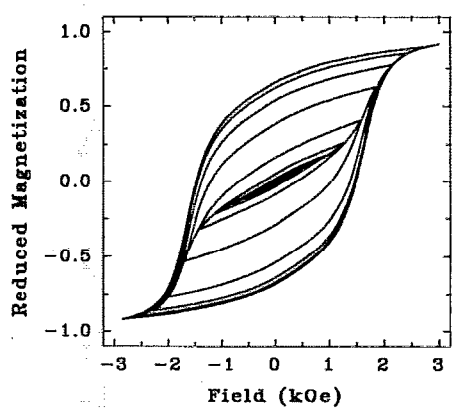

FIG. 4. Minor loops measured at room temperature for a field demagnetized sample.

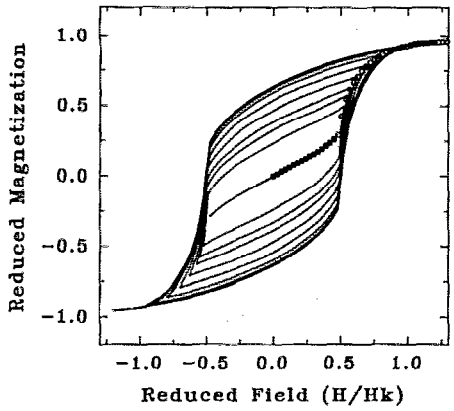

FIG. 5. Calculated minor loops and initial curve by using the Stoner–Wohlfarth model for 2-D randomly oriented noninteracting single-domain particles of uniaxial anisotropy.

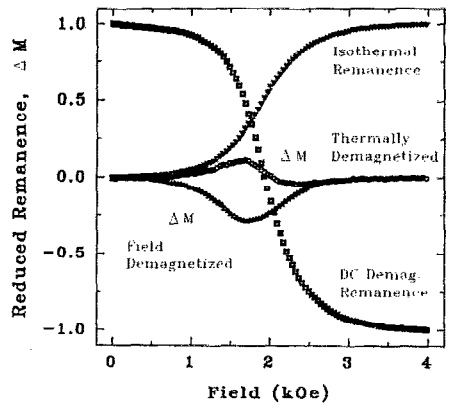

FIG. 6. Room temperature isothermal and dc demagnetization remanence curves and the ΔM curve for thermally demagnetized state and a ΔM curve for field-demagnetized sample.

In order to compare with the Stoner–Wohlfarth model[9] for rotation mechanism, we carried out a numerical calculation for 2-D (two-dimensional) and 3-D randomly oriented Stoner–Wohlfarth particles. In the 2-D case the applied field is in the plane in which the easy axes of the particles are distributed randomly. The 2-D results are used for comparison because of the nature of the film texture as discussed earlier. The calculated 2-D minor loops including the initial curve is shown in Fig. 5. The calculation has been tested by comparing the current calculated results especially in the 3-D case with the calculated results from the literature.[4,8] The agreement is excellent. There are many similarities between the 2-D calculated minor loops and initial curve and the measured results shown in Fig. 4 but they are not identical. The difference could be due to the interactions among the grains, the effect of incoherent rotation and the inhomogeneities such as a distribution of grain size and shape.

It is becoming widely accepted that the interaction among single-domain particles of uniaxial anisotropy can be estimated by measuring the deviation term ΔM from the Hankel plot predicted by Wohlfarth[10] for noninteracting single-domain particles of uniaxial anisotropy[11]:

$$\Delta M(H) = M_d(H) + 2M_r(H) - M_d(\infty), \qquad (2)$$

M_d is the so-called dc demagnetization remanence obtained after progressive demagnetizing a positively saturated sample. M_r is the isothermal remanence obtained after progressive magnetizing of an initially demagnetized sample. The two measured remanence curves and one ΔM curve calculated by using Eq.(2) for a thermally demagnetized sample are shown in Fig. 6. There is a small positive peak on the ΔM curve, suggesting a weak ferromagnetic-exchange coupling among the grains. Also shown in Fig. 6 is a ΔM curve for the same sample after demagnetization by a decreasing ac field. Now there is a negative peak, implying that magnetostatic interaction dominates over the exchange interaction. This difference between thermally demagnetized and field-demagnetized samples is observed for a number of our films. Differences in ΔM have been observed also by El-Hilo *et al.* for field-demagnetization processes with different rates.[12] One possible explanation is that the field-demagnetized state has larger regions within which grains are magnetically oriented, so that the change of ferromagnetic-exchange interaction occurs on a smaller total surface area between the larger regions. Further investigation to clarify this is under way.

We are grateful for the financial support by the DOE under grant of DE-FG02-86ER45262.

[1] H. J. Lee, J. Appl. Phys. **63**, 3269 (1988).
[2] K. Ouchi, IEEE Trans. Magn. **MAG-26**, 24 (1990); K. Hono, B. Wong, and D. E. Laughlin, J. Appl. Phys. **68**, 4734 (1990); R. D. Fisher, M. R. Khan, N. Heiman, and C. W. Nelson, IEEE Trans. Magn. **MAG-26**, 109 (1990).
[3] D. Wang and D. J. Sellmyer, J. Appl. Phys. **70**, 6053 (1991) and D. Wang, D. J. Sellmyer, and G. C. Hadjipanayis, J. Appl. Phys. **69**, 4541 (1991).
[4] B. D. Cullity, *Introduction to Magnetic Materials* (Addison-Wesley, Reading, Massachusetts, 1972), p. 310.
[5] J. S. Cook and P. L. Rossiter, CRC Crit. Rev. Solid State Mater. Sci. **15**, 543 (1989).
[6] T. Suzuki, H. Notarys, D. Dobertin, C. J. Lin, D. Weller, D. Miller, and G. Gorman, IEEE Trans. Magn. **MAG-28**, 2754 (1992), and references therein.
[7] H. Kronmüller, K. D. Durst, and M. Sagawa, J. Magn. Magn. Mater. **74**, 291 (1988).
[8] M. Sagawa, S. Hirosawa, H. Yamamoto, S. Fujimura, and Y. Matsuura, Jpn. J. Appl. Phys. **26**, 785 (1987).
[9] W. C. Stoner and W. P. Wohlfarth, Philos. Trans. R. Soc. London **240**, 599 (1948).
[10] E. P. Wohlfarth, J. Appl. Phys. **29**, 595 (1958).
[11] P. I. Mayo, K. O'Grady, R. W. Chantrell, J. A. Cambridge, I. L. Sanders, T. Yogi, and J. K. Howard, J. Magn. Magn. Mater. **95**, 109 (1991) and E. M. T. Velu and D. N. Lambeth, IEEE Trans. Magn. **MAG-28**, 3249 (1992).
[12] M. El-Hilo, K. O'Grady, P. I. Mayo, R. W. Chantrell, I. L. Sanders, and J. K. Howard, IEEE Trans. Magn. **MAG-28**, 3282 (1992).